

Tracer-based investigation of organic aerosols in marine atmospheres from marginal seas of China to the northwest Pacific Ocean

Tianfeng Guo¹, Zhigang Guo¹, Juntao Wang², Jialiang Feng^{3*}, Huiwang Gao^{2,4}, Xiaohong Yao^{2,4*}

¹ Shanghai Key Laboratory of Atmospheric Particle Pollution and Prevention, Department of Environmental Science and Engineering, Fudan University, Shanghai 200433, China;

² Lab of Marine Environmental Science and Ecology, Ministry of Education, Ocean University of China, Qingdao 266100, China

³ School of Environmental and Chemical Engineering, Shanghai University, Shanghai 200444, China

⁴ Pilot National Laboratory for Marine Science and Technology (Qingdao), Qingdao, China

Correspondence to: Xiaohong Yao (xhyao@ouc.edu.cn); Jialiang Feng (fengjialiang@shu.edu.cn)

Abstract. We investigated the geographic distributions of organic tracers in total suspended particles over marginal seas of China, including the Yellow and Bohai seas (YBS) and the South China Sea (SCS), and the northwest Pacific Ocean (NWPO) in spring, when Asian outflows strongly affect downwind marine atmospheres. The comparison of levoglucosan observed in this study with values from the literature showed that the concentrations of biomass burning aerosols over the NWPO increased largely in 2014. More observations together with our snapshot measurement, however, need to confirm whether the large increase occurred continuously through the last decades. The increase led to a mean value of levoglucosan (8.2 ± 14 ng/m³) observed over the NWPO close to that over the SCS (9.6 ± 8.6 ng/m³) and almost half of that over the YBS (21 ± 11 ng/m³). Small geographic differences in monoterpene-derived and sesquiterpene-derived secondary organic tracer concentrations were obtained among the three atmospheres, although the causes may differ. By contrast, a large difference in isoprene-derived secondary organic tracer concentrations was observed among the three atmospheres, with the sum of tracer concentrations over the SCS (45 ± 54 ng/m³) several times and approximately one order of magnitude greater than that over the YBS (15 ± 16 ng/m³) and the NWPO (2.3 ± 1.6 ng/m³), respectively. The geographic distribution of aromatic-derived secondary organic tracers was similar to that of isoprene-derived secondary organic tracers, with a slightly narrower difference, i.e., 1.8 ± 1.7 ng/m³, 1.1 ± 1.4 ng/m³ and 0.3 ± 0.5 ng/m³ over the SCS, the YBS and the NWPO, respectively. We discuss the causes of the distinctive geographic distributions of these tracers and present the tracer-based estimation of organic carbon.

1 Introduction

Aerosols that emanate from biomass burning (BB) consist primarily of carbonaceous components and inorganic salts, which can affect the climate directly by absorbing solar radiation or indirectly by acting as either cloud condensation nuclei (CCN) or ice nuclei (IN) (Bougiatioti et al., 2016; Chen et al., 2017; Hsiao et al., 2016). High BB aerosol emissions zones include boreal forests (e.g., in Eurasia and North America), tropical forests (e.g., in southeast Asia and the tropical Americas), and agriculture areas where crop residuals are burned (e.g., in developing countries such as China and India, etc.) (van der Werf et al., 2006). BB aerosols can undergo

39 long-range transport in the atmosphere, which can carry them from the continents to the oceans (Ding et al.,
40 2013; Fu et al., 2011; Kanakidou et al., 2005). For example, BB aerosols from boreal forest wildfires in Russia
41 and China reportedly made an appreciable contribution to atmospheric particle loads observed over the Arctic
42 Ocean and northwestern Pacific Ocean (NWPO) based on specific tracers of BB (Ding et al., 2013). Although
43 open wildfires from forests occur sporadically in terms of strength and occurrence frequency, global warming
44 could be conducive to vegetation fires (Running, 2006) and thus increase emissions of BB aerosols. In this
45 century, nine years were among the ten hottest global years on record, with 2014–2018 being ranked as the top
46 five hottest years (<https://www.climatecentral.org/gallery/graphics/the-10-hottest-global-years-on-record>). The
47 question is automatically raised: how do BB aerosols in the marine atmosphere in the hottest global years
48 change against those observations previously reported?

49 In addition to BB aerosols, secondary oxidation of biogenic volatile organic compounds (BVOCs) and
50 anthropogenic VOCs (AVOCs) also contribute to the particulate carbonaceous components of marine
51 atmospheres (Kanakidou et al., 2005). Secondary organic aerosols (SOAs) arising from the oxidation of
52 phytoplankton-derived isoprene have been argued to affect the chemical composition of marine atmospheric
53 aerosols and consequently impact CCN loading and cloud droplet number concentrations (Ekström et al., 2009;
54 Meskhidze and Nenes, 2006), but the importance of the marine isoprene-derived SOA is still debated (Arnold et
55 al., 2009; Claeys et al., 2010; Gantt et al., 2009; Guenther et al., 1995). For example, Gantt et al. (2009)
56 estimated that the contribution of marine isoprene-derived SOA to the OC in marine atmospheric particles is
57 <0.2% on a global scale, but that the hourly-averaged sub-micron OC emission may approach 50% over vast
58 regions of the oceans during the midday hours when isoprene emissions are highest. Several modeling studies
59 have shown that the NWPO may experience the greatest increases in sea surface temperature and CO₂ input
60 under a future warming climate (John et al., 2015; Lauvset et al., 2017). The Kuroshio Extension current system
61 leads the NWPO to be an active subtropical cyclone basin, promoting biogenic activities (Hu et al., 2018). From
62 the perspective of global change, it is a long-term need to study the dynamic changes in atmospheric aerosols
63 derived from marine sources over the NWPO and adjacent marginal seas of China, as well as their potential
64 effects on climate.

65 More importantly, BVOCs emitted from continental ecosystems and their oxidation products can significantly
66 affect the atmosphere in remote marine areas through long-range transport (Ding et al., 2013; Fu et al., 2011; Hu
67 et al., 2013a; Kang et al., 2018; Kawamura et al., 2017). BVOCs consist primarily of isoprene, monoterpenes,
68 sesquiterpenes, and their oxygenated hydrocarbons such as alcohols, aldehydes, and ketones (Ehn et al., 2014;
69 Guenther et al., 2006) and account for the majority of the global VOC inventory (Heald et al., 2008; Zhu et al.,
70 2016a, b). However, emission fluxes and oxidation processes of BVOCs show great variation, depending on
71 global warming and other factors such as regional landscape, other pollutants in the ambient air, etc. (Ait-Helal
72 et al., 2014; Claeys et al., 2004; Hu and Yu, 2013; Peñuelas and Staudt, 2010). Unlike a potential increase in
73 BVOC-derived organics aerosols in marine atmospheres under global warming, anthropogenic VOCs and
74 carbonaceous particles over the continents have been decreased because of effective mitigation of air pollutants
75 in the last decades (Li et al., 2019; Murphy et al., 2011; Sharma et al., 2004; Zhang et al., 2012). In the northern
76 hemisphere, marine atmospheres are also usually affected by anthropogenic pollutants to some extent, most of
77 which are derived from long-range transport from continents (Bao et al., 2018; Kang et al., 2019; Zhang et al.,
78 2017). The reverse trends in BVOC and anthropogenic VOC would change the composition, sources of
79 carbonaceous particles in marine atmospheres. Updated observations are thereby needed to reveal the change
80 and service the future study of the impacts.

81 In this study, we determined the concentrations of some typical organic tracers in aerosol samples obtained from
82 three cruise campaigns from the marginal seas of China, including in the South China Sea (SCS) in 2017,

83 Yellow Sea and Bohai Sea (YBS), to the NWPO in 2014, both in springtime. We investigated the influences of
84 BB aerosols from continents over three marine atmospheres, quantified the contributions of various precursors
85 to the observed SOA in marine atmospheres using organic tracers established in the literature, and explored the
86 formation pathways of SOA from their precursors during long-range transport in these hottest global years.
87 Particularly, we conducted a comprehensive comparison of this observation with those reported in literature in
88 terms of long-term variations and geographic distributions of these tracers, etc.

89 **2 Materials and Methods**

90 Total suspended particulate (TSP) samples were collected over the NWPO from 19 March to 21 April 2014,
91 over the YBS from 30 April to 17 May 2014, and over the SCS from 29 March to 4 May 2017. All samples were
92 collected on the upper deck of the R/V Dong Fang Hong II, which sits ~8 m above the sea surface. To avoid
93 contamination from the ship's exhaust, samples were collected only when the ship was sailing, and the wind
94 direction ranged from -90° to 90° relative to the bow. TSP samples were collected on quartz fiber filters
95 (Whatman QM-A) that had been pre-baked for 4 h at 500°C prior to sampling using a high-volume sampler
96 (KC-1000, Qingdao Laoshan Electric Inc., China). The sampling duration was 15–20 h at a flow rate of ~ 1000 L
97 /min. After sampling, the sample filters were wrapped in baked aluminum foil and sealed in polyethylene bags,
98 then stored at -20°C and transported to the laboratory. Field blanks were collected during each sampling period.
99 However, one sampler was out of service during the cruise on the SCS. As a compromise, cellulose filters
100 (Whatman 41) previously intended for elemental analyses were used for analyses of the organic tracers in TSP.

101 The method for determining the concentrations of tracers was adapted from Kleindienst et al. (2007) and Feng et
102 al. (2013). Briefly, 20 mL dichloromethane/methanol (1:1, v/v) was used for ultrasonic extraction of 40 cm^2 of
103 each filter at room temperature three times. The combined extracts were filtered, dried under a gentle stream of
104 ultrapure nitrogen, and then derivatized with 100 μL N,O-bis-(trimethylsilyl)-trifluoroacetamide (BSTFA,
105 containing 1% trimethylchlorosilane as a catalyst) and 20 μL pyridine at 75°C for 45 min. Gas chromatography
106 mass spectrometry (GC-MS) analyses were conducted with an Agilent 6890 GC/5975 MSD. Prior to solvent
107 extraction, methyl- β -D-xylanopyranoside (MXP) was spiked into the samples as an internal/recovery standard.
108 Hexamethylbenzene was added prior to injection as an internal standard to check the recovery of the surrogates.
109 Like those reported by Feng et al. (2013), the primary organic tracers measured in this study included
110 levoglucosan (LEVO), mannosan, and galactosan. Four types of secondary organic tracers were used:
111 isoprene-derived secondary organic tracers (SOA_I) including 2-methylglyceric acid (2-MGA), C5-alkene triols
112 (cis-2-methyl-1,3,4-trihydroxy-1-butene, 3-methyl-2,3,4-trihydroxy-1-butene and
113 trans-2-methyl-1,3,4-trihydroxy-1-butene), and MTLs (2-methylthreitol and 2-methylerythritol);
114 monoterpene-derived secondary organic tracers (SOA_M) including 3-hydroxyglutaric acid (HGA),
115 3-hydroxy-4,4-dimethylglutaric acid (HDMGA), and 3-methyl-1,2,3-butanetricarboxylic acid (MTBCA); the
116 sesquiterpene-derived secondary organic tracer (SOA_S) β -caryophyllinic acid; and the aromatic
117 (toluene)-derived secondary organic tracer (SOA_A) 2,3-dihydroxy-4-oxopentanoic acid (DHOPA). LEVO was
118 quantified based on authentic standards in this study. While the SOA tracers without available commercial
119 standards were quantified using methyl- β -D-xylanopyranoside (MXP) as a surrogate. To reduce the uncertainty
120 of quantification, relative response factors of the target tracers to MXP were estimated by comparing the area
121 ratio of typical target ions to MXP to that of total ions in selected samples that showed high concentrations of
122 the target tracers (Feng et al., 2013).

123 Field blanks and laboratory blanks (ran every 10 samples) were extracted and analyzed in the same manner as
124 the ambient samples. Target compounds were nearly always below the detection limit in field and laboratory
125 blanks. Recoveries of the surrogate (MXP) were in the range of 70–110%. The reported results were corrected

126 for recovery, assuming that the target compounds had the same recovery as the surrogate. Duplicate analyses
127 indicated that the deviation was less than 15%.

128 However, the substitution of cellulose filters (Whatman 41) during the cruise on the SCS led to increased field
129 blank values for some tracers. The tracer concentrations in those samples were, however, over three times higher
130 than the field blank values, except for those of mannosan and galactosan. Data for mannosan and galactosan
131 were thus not available, nor were the total organic carbon concentrations, for samples collected during the cruise
132 on the SCS.

133 The concentrations of organic carbon (OC) and element carbon (EC) in each sample were measured with a DRI
134 2001A thermal/optical carbon analyzer (Atmoslytic Inc., Calabasas, CA, USA) using the IMPROVE
135 temperature program (Wang et al., 2015). All filters before and after sampling were weighted at a glovebox
136 under controlled ambient temperature and relative humidity. Mass concentrations of TSP, however, should be
137 treated as semi-quantitative results by considering analytic errors of quartz fiber filters (Yao et al., 2009).

138 3. Results and Discussion

139 3.1 Spatiotemporal distributions of LEVO

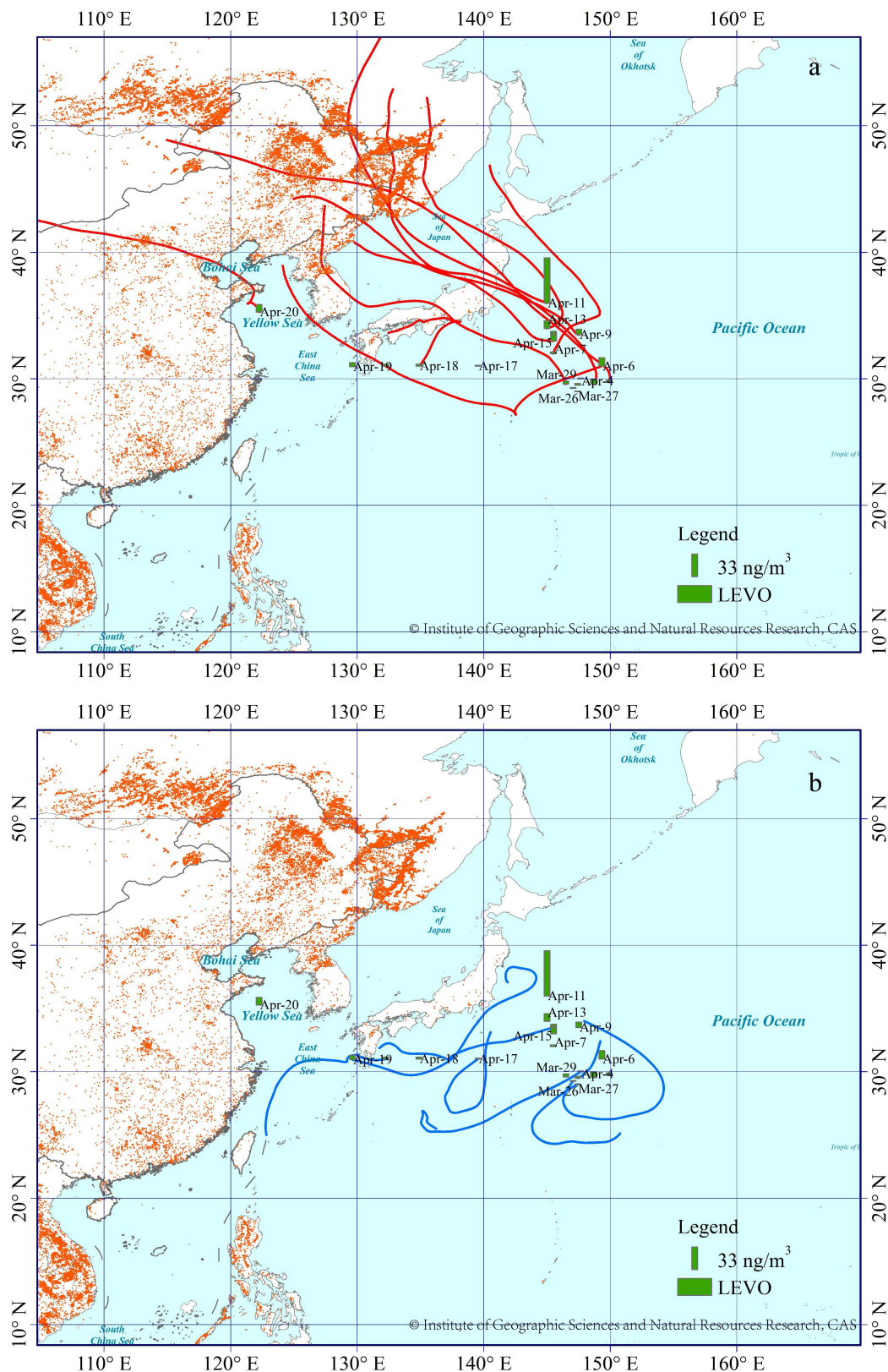
140 Levoglucosan, mannosan, and galactosan produced by the pyrolysis of cellulose and hemicellulose have been
141 widely used as organic tracers of BB aerosols in ambient air (Ding et al., 2013; Fu et al., 2011; Feng et al.,
142 2013). The mean levels of LEVO in TSP collected during the cruises on the NWPO and the SCS were
143 comparable, at 8.2 ng/m³ and 9.6 ng/m³, respectively (Figure S1, Table 1). They were almost half of the mean
144 value of 21 ng/m³ during the cruise on the YBS, where high concentrations of BB aerosols have been observed
145 in continental atmospheres upwind of the YBS mainly from wildfires and the burning of crop residue, wildfire,
146 etc. (Feng et al., 2012; Feng et al., 2013; Yang et al., 2014). Unlike the small difference among the mean values,
147 the concentration of LEVO fluctuated greatly among TSP samples in each oceanic zone, ranging from 0.5 to 65
148 ng/m³ over the NWPO, from 1.0 to 30 ng/m³ over the SCS and from 2.5 to 42 ng/m³ over the YBS (Fig. S1).
149 High spatiotemporal variation in LEVO in TSP has also been observed in literature, with concentrations of
150 LEVO fluctuating around 0.2–41 ng/m³ during Arctic to Antarctic cruises from July to September 2008 and
151 from November 2009 to April 2010 (Hu et al., 2013b). Hu et al. (2013b) also reported the highest LEVO
152 concentrations occurring at mid-latitudes (30°–60° N and S) and the lowest at Antarctic and equatorial latitudes
153 over the several months of sampling. This distinctive geographical distribution was not observed in the present
154 study, as there were no significant differences in LEVO in TSP between the SCS and NWPO ($P > 0.05$).

155 Narrow spatiotemporal variation in LEVO in TSP has been reported during summer sampling over the North
156 Pacific Ocean and the Arctic in 2003, with maximum and mean values as low as 2.1 ng/m³ and 0.5 ng/m³,
157 respectively (Ding et al., 2013). A lower mean value of LEVO of 1.0 ng/m³ has also been reported in the spring
158 over the island of Chichi-jima from 2001 to 2004 (Mochida et al., 2010), while the levels increased to 3.1 ± 3.7
159 ng/m³ in TSP collected on the island of Okinawa in 2009–2012 (Zhu et al., 2015). Using these previous
160 observations as a reference (Table 1), our observations suggest that the BB aerosols from the long-range
161 transport over the NWPO in 2014 largely increased. Thus, an important question is raised, i.e., does the increase
162 occur continuously and largely over the last decades in marine atmospheres over the NWPO? Due to the lack of
163 BB sources in oceans, large spatiotemporal variation in the concentrations of LEVO in the marine atmosphere
164 may be related to the long-range transport of atmospheric particles from continents. Thus, 72 h back trajectories
165 of air masses at a height of 1000 m during our sampling periods (Figs. 1, 2) were calculated using the HYSPLIT
166 model (<https://ready.arl.noaa.gov/HYSPLIT>). Based on the calculated back trajectories, TSP samples could be

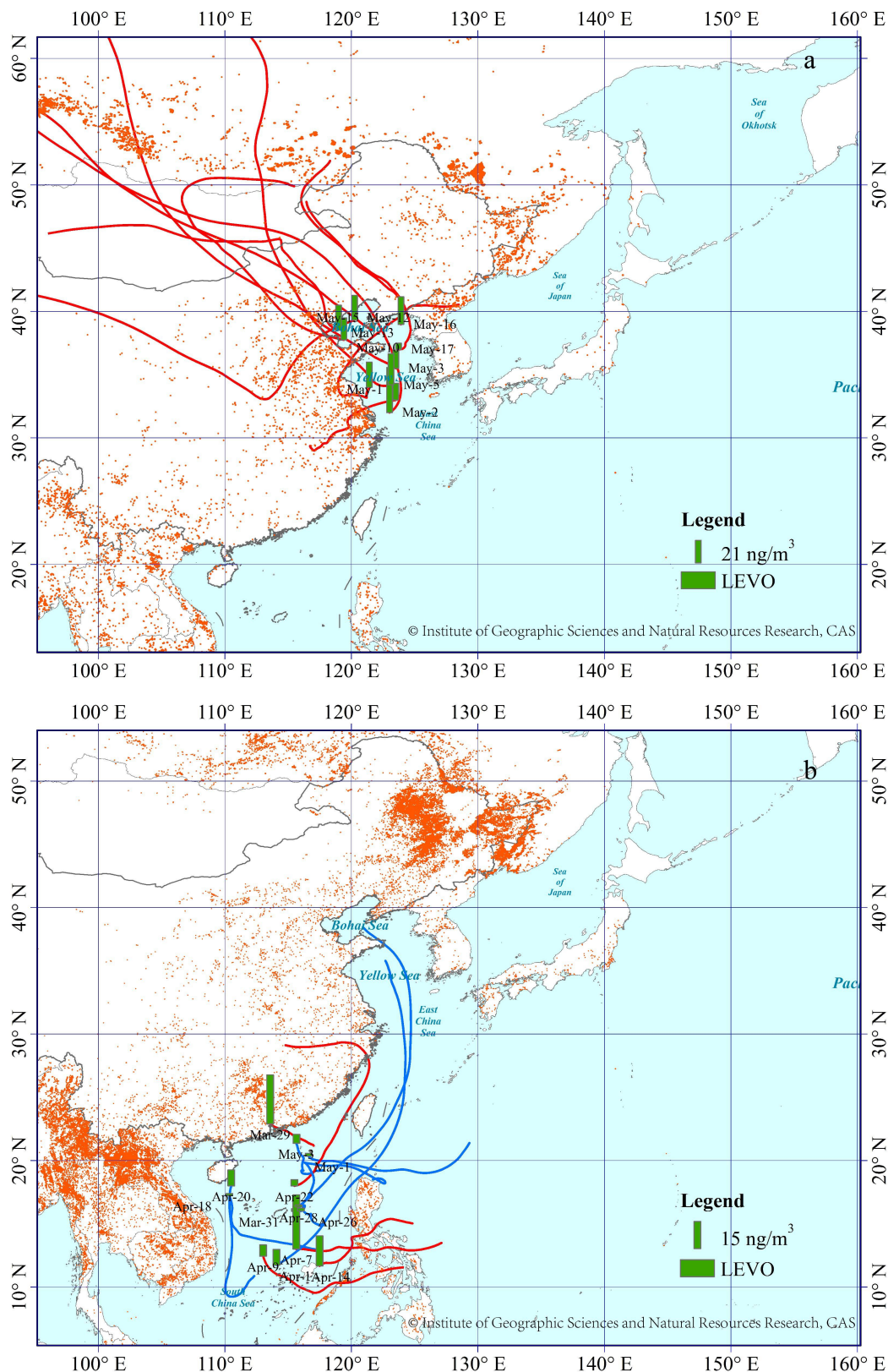
167 classified into two categories with Category 1 representing continent-derived aerosol samples and Category 2
168 being ocean-derived aerosol samples. All 12 samples collected over the YBS fell into Category 1 (Fig. 2). Half
169 (11/19) of the samples collected over the NWPO were classified into Category 1 (Fig. 1). A significant
170 difference ($p < 0.05$) was obtained between the concentrations of LEVO in Category 1 ($13 \pm 18 \text{ ng/m}^3$) and
171 Category 2 ($2.0 \pm 1.8 \text{ ng/m}^3$) over the NWPO. The values in Category 2 were closer to the springtime
172 observations reported by Mochida et al. (2010) and Zhu et al. (2015) as well as the summer observations
173 reported by Ding et al. (2013), reflecting the marine background value less affected by continental air masses.
174 On the other hand, the much higher values in Category 1 than Category 2 further indicate a large increase in
175 contribution of BB aerosols being transported from the continents to the remote marine atmosphere in 2014.
176 On 11 April 2014 over the NWPO, an episode of high LEVO concentration of 65 ng/m^3 occurred (Fig. 1). Like
177 LEVO, the concentrations of galactosan and mannosan in the sample were also the highest among all samples
178 collected over the NWPO. This sample was collected in the oceanic zone, approximately 500 km from the
179 continent of Japan. A combination of air mass back trajectories and NASA's FIRMS Fire Map indicated strong
180 BB aerosol emissions from intense fire events in Siberia, followed by long-range transport with the westerly
181 wind as the major contributors to this anomaly (Fig. 1). A similar episodic concentration of LEVO of 27 ng/m^3
182 in TSP was observed once previously over the NWPO during a circumnavigation cruise (Fu et al., 2011). By
183 combining satellite data with other observations, many studies in literature have found that BB aerosols from
184 major forest fires and smoke events in Siberia could be transported downwind to remote marine regions not only
185 in spring, but also in summer (Ding et al., 2013; Generoso et al., 2007; Huang et al., 2009). In a few cases, BB
186 aerosols have been reported to have reached as far as the adjacent Arctic region (Generoso et al., 2007; Warneke
187 et al., 2010). Van der Werf et al. (2006) estimated the emissions of BB aerosols from Eurasia to be much larger
188 than those from North America. Thus, it is not surprising that the concentrations of LEVO over the NWPO were
189 much higher than those over the eastern North Pacific and western North Atlantic at similar latitudes (Hu et al.,
190 2013b).

191 In addition, both galactosan and mannosan showed strong linear correlations with LEVO ($R^2 = 0.98$, $p < 0.05$)
192 in TSP collected over the NWPO and YBS in this study. These strong correlations indicate that the three tracers
193 were probably derived from the same BB sources. Previous studies have reported LEVO/mannosan (L/M) ratios
194 of 3–10, 15–25, and 25–40 from softwood, hardwood, and crop-residue burning, respectively (Kang et al., 2018;
195 Zhu et al., 2015). The calculated L/M ratios in TSP collected over the NWPO were 19 ± 4 in this study, which
196 implies dominant contributions from herbaceous plants and hardwood. The calculated L/M ratios in TSP
197 collected over the YBS were 14 ± 11 , indicating mixed sources.

198 In all, 5 of 13 samples collected over the SCS were classified into Category 1, with air masses identified as
199 originating from either the continental areas of South China or the Philippines (Fig. 2). The concentration of
200 LEVO fluctuated around $17 \pm 12 \text{ ng/m}^3$ in Category 1 but decreased to $3.6 \pm 3.4 \text{ ng/m}^3$ in Category 2. However, no
201 significant difference was found between categories due to the large variation in LEVO concentration among the
202 limited number of samples in Category 1 ($p > 0.05$). Forest fires occur accidentally, leading to the large variation
203 in LEVO in Category 1. Southern Asia has been reported to be one of the greatest emission sources of BB
204 aerosols worldwide (van der Werf et al., 2006), which likely led to the higher mean value of LEVO in Category
205 1. However, the LEVO level observed over the SCS in Category 2 was closer to that reported from low-latitude
206 regions ($2.7 \pm 1.1 \text{ ng/m}^3$, Table 1) collected during a global circumnavigation cruise (Hu et al., 2013b). Hu et al.
207 (2013b) argued that their low observed concentrations may have been associated with intense wet deposition,
208 degradation as well as intensive moist convection that occurred in the tropical region during their summer cruise.
209 Unfortunately, no previous observations of LEVO in spring can allow us analyzing the long-term variation in
210 contribution of BB aerosols therein. However, this observation can be used for future comparison.



211
 212 **Figure 1. Spatial distribution of LEVO in TSP over the NWPO in spring of 2014 and 72-hrs back**
 213 **trajectory associated with each TSP sample. The red lines represent that air masses can be derived from**
 214 **the continent (a, Category 1); the blue lines represent that air masses may be derived mainly from the**
 215 **oceans (b, Category 2). The red dots represent the locations of fires from Fire Information for Resource**
 216 **Management System (FIRMS, <https://firms.modaps.eosdis.nasa.gov/>).** And the base map was from
 217 **Resource and Environment Data Cloud Platform (<http://www.resdc.cn/DOI>), DOI: 10.12078/2018110201,**
 218 **© Institute of Geographic Sciences and Natural Resources Research, Chinese Academy of Sciences (CAS).**
 219 **The data from Resource and Environment Data Cloud Platform are open and free.**



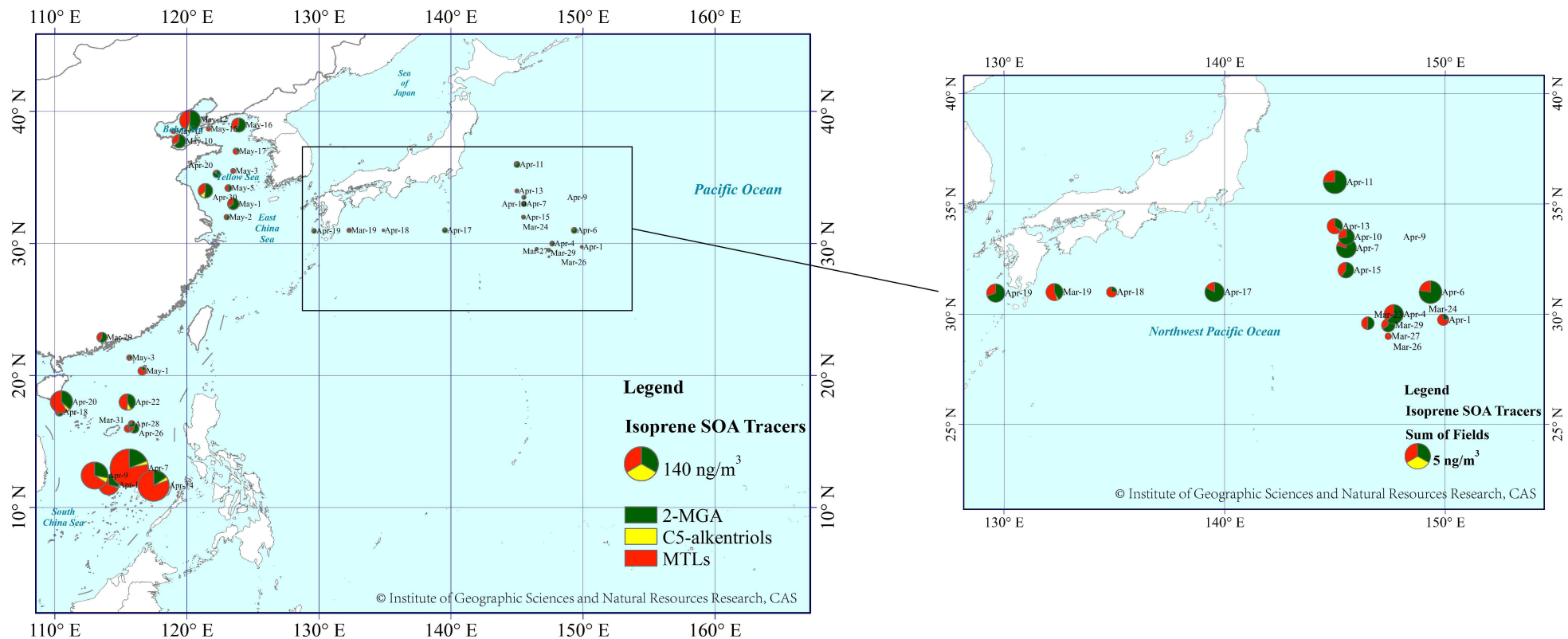
220
 221 **Figure 2. Spatial distribution of LEVO over the YBS (a, 2014), and SCS (b, 2017), detailed information**
 222 **described in Figure 1. And the base map was from Resource and Environment Data Cloud Platform**
 223 **(<http://www.resdc.cn/DOI>), DOI: 10.12078/2018110201, © Institute of Geographic Sciences and Natural**
 224 **Resources Research, Chinese Academy of Sciences (CAS).**

225 3.2 Spatiotemporal distributions of SOA_I tracers

226 SOA_I tracers were detected during all three cruises. The sum of SOA_I tracers showed a decreasing trend of up to

227 approximately one order of magnitude from marginal seas to the open ocean, i.e., $45 \pm 54 \text{ ng/m}^3$ in TSP over the
228 SCS, $15 \pm 16 \text{ ng/m}^3$ over the YBS and $2.3 \pm 1.6 \text{ ng/m}^3$ over the NWPO (Fig. S1). The highest sum value of SOA_I
229 tracers over the SCS was 176 ng/m^3 , indicating strong photochemical formation of SOA from biogenic volatile
230 organics (Fig. 3). The geographical distribution of SOA_I tracers in this study was generally consistent with those
231 reported by Hu et al. (2013a), with higher concentrations of these tracers in atmospheric particles collected from
232 low-latitude oceanic zones (30° S – 30° N) due to large emissions from tropical forests and strong photochemical
233 reactions. Their reported average contents of SOA_I tracers in low-latitude oceanic zones fluctuated around
234 $9.2 \pm 6.7 \text{ ng/m}^3$, much lower than those measured in this study.

235 When the sum of SOA_I tracers in each sample was examined separately according to the air mass source, a
236 significant difference was found over the SCS between Category 1 ($85 \pm 66 \text{ ng/m}^3$) and Category 2 (19 ± 22
237 ng/m^3), with significance at $p < 0.01$. The average contribution of SOA_I tracers to TSP mass concentration over
238 the SYS was higher in category 1 ($0.4\% \pm 0.6\%$) than in category 2 ($0.06\% \pm 0.07\%$). The tracer values were
239 $2.7 \pm 1.8 \text{ ng/m}^3$ in Category 1 and $1.7 \pm 1.0 \text{ ng/m}^3$ in Category 2 over the NWPO, where no significant difference
240 between the two categories was found ($p > 0.05$). The average contribution of SOA_I tracers to TSP mass
241 concentration over the NWPO was higher in category 1 ($0.008\% \pm 0.005\%$) than that in category 2 ($0.005\% \pm$
242 0.005%). Supposed that concentrations of the tracers in Category 2 were completely contributed by marine
243 sources, it can be inferred that SOA_I carried by continental air masses increased sharply over the SCS. However,
244 it was not the case over the NWPO. Because all samples over the YBS fell into Category 1, this comparison
245 could not be made for the YBS.



246
 247 **Figure 3. Spatial distribution of SOA₁ tracer compounds over three marine regions, YBS and NWPO in 2014, SCS in 2017. The area of the pie indicates the concentration of total**
 248 **SOA₁ tracers. And the base map was from Resource and Environment Data Cloud Platform (<http://www.resdc.cn/DOI>), DOI: 10.12078/2018110201, © Institute of Geographic**
 249 **Sciences and Natural Resources Research, Chinese Academy of Sciences (CAS).**

250 3.3 Spatiotemporal distributions of SOA_M, SOA_s tracers

251 The sum of SOA_M tracers including HGA, HD-MGA, and MBTCA was greatest over the SCS region (3.5±6.0
252 ng/m³), where the concentration was approximately double that over the YBS (1.6±2.0 ng/m³) and NWPO
253 regions (1.6±2.7 ng/m³) (Fig. S1), but no significant differences were identified between any two campaigns.
254 The concentrations of SOA_M tracers were almost one magnitude lower than those of SOA_I tracers. Due to the
255 unique contribution of terpene-derived SOA to nucleation and growth of newly formed particles in the
256 atmosphere (Ehn et al., 2014; Gordon et al., 2017; Zhu et al., 2019), the SOA_M may primarily cause indirect
257 climate effects rather than direct effects of aerosols in the marine atmosphere. The difference in mean SOA_M
258 concentration between the SCS and NWPO narrowed to a factor of two, in contrast to the differences of
259 approximately one order of magnitude in mean SOA_I between the two types of atmospheres. The precursors of
260 SOA_M tracers derive mainly from coniferous forests (Duhl et al., 2008) and the decreasing proportion of
261 coniferous forests in subtropical and tropical regions may partially explain the smaller spatial difference in
262 SOA_M tracers over the SCS compared to the YBS and NWPO. However, the comparable SOA_M levels over the
263 YBS and NWPO have not yet been explained.

264 Only three SOA_M tracers were measured in this study, but other SOA_M tracers have been measured and reported
265 in marine atmospheres (Fu et al., 2011; Kang et al., 2018). In order to compare our results with the total amount
266 of SOA_M tracers in the literature, the total amounts measured in this study were multiplied by a factor of 3.1
267 (described in supporting information Sect. S1, Fig. S4) according to the chamber results obtained by Kleindienst
268 et al. (2007). The adjusted values over the SCS were closer to the mean of 11.6 ng/m³ observed over the East
269 China Sea (ECS) (Kang et al., 2018) and the lower values of 9.80–49.0 ng/m³ observed among 12 continental
270 sites in China (Ding et al., 2016). The adjusted total amounts of SOA_M over the NWPO and YBS were
271 comparable to previous observations of 3.0±5.0 ng/m³ collected from the Arctic to Antarctic in 2008-2010 (Hu
272 et al., 2013a), but much higher than observations of 63±49 pg/m³ over the North Pacific and Arctic in 2003
273 (Ding et al., 2013). This may also imply a substantial increase in SOA_M in the last decades, although more
274 investigations are needed to confirm this.

275 β-Caryophyllene is a major sesquiterpene emitted from plants such as Scots pine and European birch (Duhl et al.,
276 2008; Tarvainen et al., 2005). β-Caryophyllinic acid is formed through the ozonolysis or photo-oxidation of
277 β-caryophyllene. The highest levels of β-caryophyllinic acid were observed over the YBS (0.13±0.03 ng/m³),
278 followed by the SCS (0.08±0.11 ng/m³) and NWPO (0.05±0.09 ng/m³) (Fig. S1). The spatial distribution of
279 β-caryophyllinic acid clearly did not follow the general trend of biogenic SOA, with the highest values over the
280 SCS followed by the YBS. Compared to values from the literature, our results are much higher than those over
281 the North Pacific and Arctic Oceans (2.4±5.4 pg/m³) (Ding et al., 2013) but much lower than observations over
282 the East China Sea reported by Kang et al. (2018), where β-caryophyllinic acid was reported to be in the range
283 of 0.16–17.2 ng/m³ with a mean of 2.9 ng/m³. The large differences in β-caryophyllinic acid content observed in
284 various campaigns remain unexplained.

285 3.4 Spatiotemporal distributions of SOA_A tracers

286 When the concentrations of DHOPA in TSP were examined, the highest concentrations occurred over the SCS
287 (1.8±1.7 ng/m³), followed by the YBS (1.1±1.4 ng/m³), and the lowest values were recorded in the NWPO
288 region (0.3±0.5 ng/m³) (Fig. S1). The decreasing extent of the DHOPA from the SCS to the NWPO was
289 approximately three times less than that of SOA_I tracers but approximately three times larger than that of SOA_M

290 tracers. Ding et al. (2017) reported annual averages of DHOPA among various sites in China, which ranged from
291 1.2 to 8.8 ng/m³. The concentrations of DHOPA observed over the SCS and the YBS were similar to the lower
292 values observed in upwind continental atmospheres.

293 Formation of DHOPA depends on the molecular structures of aromatics, as well as concentrations of free
294 radicals and oxidants, etc. (Henze et al., 2008; Li et al., 2016). The mean value of DHOPA in Category 1
295 (0.43±0.65 ng/m³) was nearly twice that in Category 2 (0.20±0.31 ng/m³) over the NWPO ($p > 0.05$). With two
296 samples with high DHOPA (1.2, 2.1 ng/m³) in Category 1 to be excluded, the recalculated average DHOPA
297 decreases down to 0.17±0.21 ng/m³. The continent-derived DHOPA seemingly yielded a minor contribution to
298 the observed values over the NWPO, except during strong long-range transport episodes. Similarly, the mean
299 values of DHOPA were same in Category 1 (1.8±2.1 ng/m³) and Category 2 (1.8±1.5 ng/m³) samples collected
300 over the SCS and no significant difference was observed between two categories. Much stronger UV radiation
301 occurs over the SCS than the YBS, which may contribute to the elevated DHOPA level over the SCS. Aside
302 from continent-derived precursors, oil exploration and heavy marine traffic over the SCS are also potential
303 contributors to the higher DHOPA levels therein, and this link requires further investigation. Previous field
304 observations in China have demonstrated that biofuel or biomass combustion emissions act as important sources
305 of aromatics in the atmosphere (Zhang et al., 2016), as evidenced by the association between the nationwide
306 increase in DHOPA during the cold period and the enhancement of BB emissions (Ding et al., 2017). In this
307 study, no linear correlation was obtained between DHOPA and LEVO in samples collected over the SCS and the
308 other two campaigns, leaving emissions other than BB emissions, e.g., solvent use, oil exploration, marine
309 traffic, etc., as the major precursors for DHOPA in these marine atmospheres (Li et al., 2014).

310 3.5 Causes for high photochemical yields of SOA_I over the SCS

311 Because higher concentrations of SOA_I were observed in TSP samples collected over the SCS, the composition
312 of SOA_I tracers was further investigated in terms of their formation pathways and sources. Based on the results
313 of chamber experiments, Surratt et al. (2010) proposed different formation mechanisms for 2-MGA and MTLs.
314 2-MGA is a C₄-dihydroxycarboxylic acid, which forms through a high-NO_x pathway. MTLs and C₅-alkene
315 triols are mainly products of the photooxidation of epoxydiols of isoprene under low-NO_x conditions.

316 MTLs acted as the dominant compounds among SOA_I tracers in most TSP samples collected over the SCS, with
317 concentrations of 31±42 ng/m³ (Fig. 3). The ratio of 2-MGA/MTLs ranged from 0.2 to 3.1, with a median value
318 of 0.6. The ratio exceeded the unity in only 4 of 13 samples. This result allowed us to infer that the observed
319 SOA_I tracers were generated mainly under low-NO_x conditions. Although the concentration of
320 2-methylerythritol was nearly double that of 2-methylthreitol, they were highly correlated ($R^2 = 0.99$, $p < 0.05$)
321 because of their shared formation pathway. Satellite data showed that the NO₂ levels in South China and the
322 Philippines were low, except in a few hotspots (Fig. S2). Such low-NO_x conditions favor the formation of
323 MTLs rather than 2-MGA over the tropical SCS. The isoprene emitted from plants growing on oceanic islands
324 may also undergo chemical conversion to SOA under low-NO_x conditions, and low-NO_x conditions are always
325 expected in remote marine atmospheres (Davis et al., 2001).

326 In general, zonally and monthly averaged OH concentrations around 15°N are ~50% were greater than those
327 around 35 °N (Bahm and Khalil, 2004). Thus, enhanced formation of MTLs is theoretically expected under the
328 strong UV radiation of tropical regions. However, no significant correlation between the concentrations of
329 MTLs and UV radiation was obtained over the SCS (data not shown) possibly due to the influences of various
330 air masses. A field study showed that MTL yields were positively correlated with ambient temperature in
331 continental atmospheres (Ding et al., 2011). 2-MGA yields, in contrast, showed no significant correlation with

332 ambient temperature in this study. Moreover, lower relative humidity may enhance the formation of 2-MGA in
333 the particulate phase but not for MTLs (Zhang et al., 2011). Variation in ambient temperature and relative
334 humidity may complicate the relationship between the concentrations of SOA_I tracers and UV radiation over the
335 SCS.

336 In addition, the MTLs concentration in Category 1 (62 ± 55 ng/m³) was larger than that in Category 2 (11 ± 14
337 ng/m³). The more abundant MTLs associated with Category 1 was most likely related to long-range transport of
338 these chemicals from upwind continental areas, the oxidation of continental precursors in the marine atmosphere,
339 or both. Large emissions of isoprene were expected from tropical forests upwind of the SCS due to the high
340 vegetation coverage and high ambient temperature of such areas (Ding et al., 2011; Rinne et al., 2002). Global
341 estimates show tropical trees to be responsible for ~80% of terpenoid emissions and ~50% of other VOC
342 emissions (Guenther et al., 2012).

343 In a clean marine atmosphere, phytoplankton is the sole source of isoprene emissions over the oceans (Bonsang
344 et al., 1992; Broadgate et al., 1997). Chlorophyll-a has been widely employed as a measure of phytoplankton
345 abundance and a proxy for predicting isoprene concentrations in water (Hackenberg et al., 2017). The
346 satellite-derived chlorophyll-a level during the study period over the SCS was below 0.45 mg/m³, excluding
347 coastal areas (Fig. S3). The MTLs observation of 11 ± 14 ng/m³ in Category 2 should be considered as the upper
348 limitation value derived from marine phytoplankton in the SCS. Although air masses differed between
349 Categories 1 and 2, a good correlation was obtained between MTLs and 2-MGA when the data in the two
350 categories was pooled for analyses ($R^2 = 0.77$, $P < 0.01$). This strong correlation indicates these tracers are
351 primarily formed through shared pathways. However, this correlation was poor over the NWPO, as discussed
352 below.

353 3.6 Origin and formation of SOA_I over the NWPO

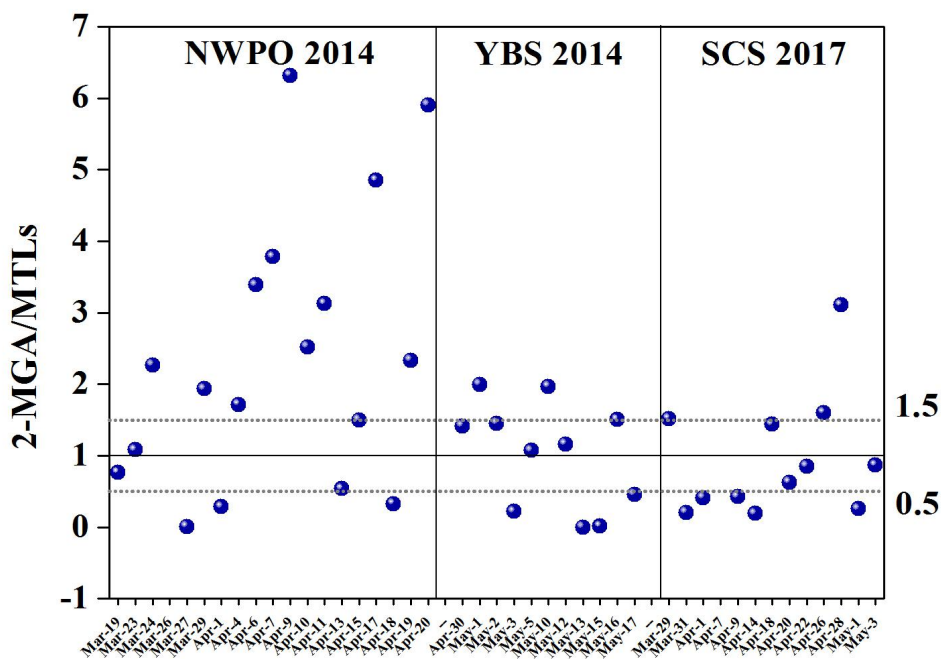
354 Over the NWPO, the concentration of 2-MGA was 1.6 ± 1.5 ng/m³, which was generally dominant among SOA_I
355 tracers, followed by MTLs (0.7 ± 0.3 ng/m³) and C5-alkene triols (0.03 ± 0.02 ng/m³). When the ratio of
356 2-MGA/MTLs was further examined, it varied greatly from <0.1 to 6.3, with a median value of 2.1. Most ratios
357 observed over the NWPO in this study were far greater than the values of 0.18–0.59 reported by Hu et al. (2013a)
358 from a global circumnavigation cruise, and also greater than 0.87–1.8 reported in urban areas of California
359 (Lewandowski et al., 2013) and the maximum value of 2.0 obtained over the YBS. Ding et al. (2013) also
360 reported ratios that fluctuated greatly from 0.5 to 10 with a median value of 3.3 during a summer cruise in the
361 NWPO and Arctic Ocean in 2003. The large 2-MGA/MTL ratios over the NWPO appeared to be highly
362 consistent over two independent sampling campaigns.

363 The compound profile of SOA_I tracers over the NWPO implied high-NO_x conditions allowing oxidation of
364 isoprene to generate the SOA_I present in most samples. Such high-NO_x conditions are impossible in a remote
365 marine atmosphere, as indicted in Figure S2. Given that the lifespan of isoprene in the atmosphere is only
366 several hours (Bonsang et al., 1992), the long-range transport of oxidation products formed under high NO_x
367 levels over the continents likely led to the 2-MGA-dominated composition of SOA_I. Based on air mass back
368 trajectories, this long-range transport may involve 2-MGA originating from Siberia, northeastern China, or
369 Japan.

370 Organic aerosols over the NWPO were strongly influenced by forest fires that take place in Siberia during
371 spring and summer almost every year (Ding et al., 2013; Huang et al., 2009). Previous emissions inventory
372 studies have reported high isoprene and NO_x emissions from various BB types (Akagi et al., 2011; Andreae and
373 Merlet, 2001). Ding et al. (2013) thus argued that an increase in emissions of isoprene in the presence of BB,

374 followed by its chemical conversion under high-NO_x conditions, may lead to transport over thousands of
 375 kilometers and hold at the detectable concentrations in the remote marine atmosphere over the NWPO. The
 376 same argument may hold true for the elevated ratios of 2-MGA/MTLs observed over the NWPO in this study
 377 (Fig. 4). However, we did not find a significant correlation between 2-MGA and LEVO over the NWPO. The
 378 decomposition of LEVO reported in literature (Fraser and Lakshmanan, 2000; Hennigan et al., 2010; Hoffmann
 379 et al., 2010) may lower the correlation between them. However, whether 2-MGA can decompose in ambient air
 380 remains poorly understood.

381 On the other hand, the ratios of 2-MGA/MTLs in 3 of 19 samples collected over the NWPO were below 0.5
 382 (Figure 4). In these cases, the oxidation of isoprene under low-NO_x conditions likely dominated the generation
 383 of SOA_I. The ratios of 2-MGA/MTLs were 0.5–1.5 in 4 of 19 samples, suggesting mixed contributions to SOA_I
 384 from the oxidation of isoprene under low-NO_x conditions and high-NO_x conditions. As the major formation
 385 pathways of 2-MGA and MTLs varied greatly among samples, no significant correlation ($R^2 = 0.12$, $p > 0.05$)
 386 was obtained between 2-MGA and MTLs over the NWPO. Recall that the tracer values of SOA_I were 2.7 ± 1.8
 387 ng/m³ in Category 1 and 1.7 ± 1.0 ng/m³ in Category 2. This implied that SOA_I derived from marine sources was
 388 comparable to that derived from the continent outflows.



389
 390 **Figure 4. Spatial ratio of 2-MGA/MTLs among SOA_I tracers over three marine regions.**

391 **3.7 Source apportionment of secondary organic carbon (SOC)**

392 The tracer-based approach developed by Kleindienst et al. (2007) was applied to estimate the concentrations of
 393 SOC and WSOC_{BB}, as follows:

$$[SOC] = \frac{\sum_i [tri]}{f_{SOC}} \quad (1)$$

$$[WSOC_{BB}] = \frac{C_{tracer}}{f_{tracer/WSOC_{BB}}} \quad (2)$$

396 where $\Sigma_i(\text{tri})$ is the sum of concentrations of the selected suite of tracers for a precursor, and f_{SOC} is the mass
397 fraction of tracer compounds in SOC generated from the precursor in chamber experiments. Assuming that the
398 f_{SOC} values in ambient air match those in the chamber, the f_{SOC} values for precursors such as isoprene,
399 monoterpenes, β -caryophyllene, and aromatics were $0.155 \pm 0.039 \mu\text{g}/\mu\text{gC}$, $0.231 \pm 0.111 \mu\text{g}/\mu\text{gC}$, 0.023 ± 0.0046
400 $\mu\text{g}/\mu\text{gC}$, and $0.00797 \pm 0.0026 \mu\text{g}/\mu\text{gC}$, respectively (Kleindienst et al., 2007), with uncertainty described in
401 Sect. S2. The fraction of LEVO in WSOC ($0.0994 \mu\text{g}/\mu\text{gC}$) from the BB plume was used for WSOC_{BB} (Ding et
402 al., 2008). The f_{SOC} value for monoterpenes was scaled up by a factor of 3.1 based on experimental observations,
403 as these two tracers (HGA+HD-MGA) accounted for 2/9 of the total tracers of monoterpenes, as described in
404 the supporting information (Kleindienst et al., 2007).

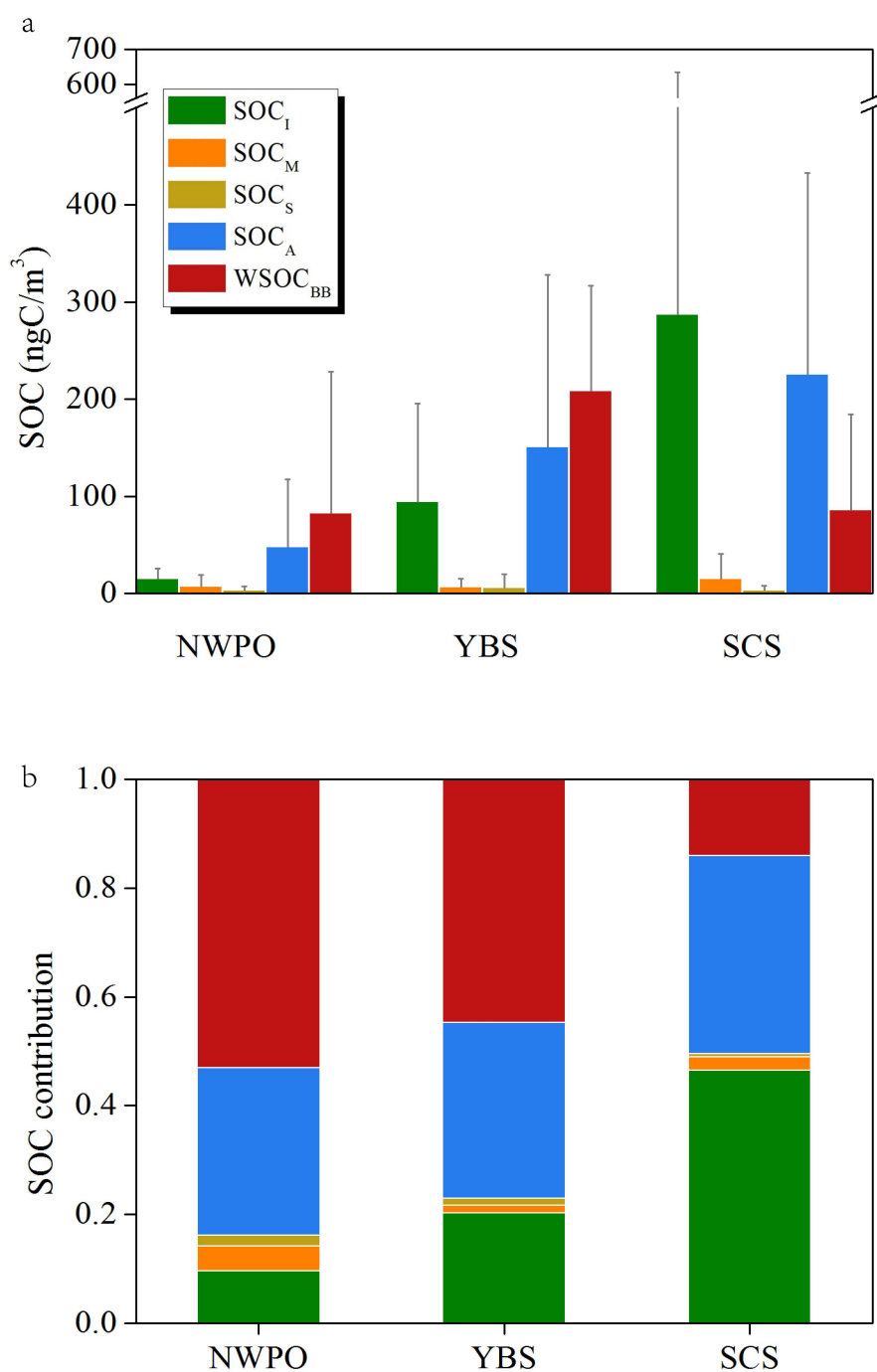
405 Over the SCS, nearly half of the sum of SOC and WSOC_{BB} was in the form of SOC_I (47%), followed by SOC_A
406 (36%), WSOC_{BB} (14%) and a minor contribution of 2.5% from SOC_M (Fig. 5). This composition pattern over
407 the SCS could be attributed to abundant biogenic SOA formation in low-latitude tropical marine atmospheres.
408 Over tropical marine regions, atmospheric oxidation products can account for 47–59% of the total organic
409 content estimated, with biomass burning emissions making up only 2–7% based on source apportionment using
410 organic tracers (Fu et al., 2011). A model study by Fu et al. (2012) showed that secondary formation accounts
411 for as much as 62% of OC estimated using tracers in eastern China in summer. A reverse pattern was observed
412 over the YBS, with WSOC_{BB} as the dominant contributor (45%) to the sum of SOC and WSOC_{BB}, followed by
413 SOC_A (32%) and SOC_I (20%). The contribution of SOC_M was also minor, at 1.5%. Notably, the chemical
414 composition observed over the NWPO was similar to that over the YBS, with WSOC_{BB} contributing up to 53%.
415 In addition, Kang et al. (2018) used the PMF method to identify various sources of OC in marine aerosols over
416 the ECS such as secondary nitrate, BSOA, BB, and fungal spores.

417 Geographically, the estimated SOC values from BVOCs ranked at the highest level of $306 \pm 343 \text{ ngC}/\text{m}^3$ over the
418 SCS, decreasing to $107 \pm 99 \text{ ngC}/\text{m}^3$ over the YBS and $24 \pm 22 \text{ ngC}/\text{m}^3$ over the NWPO. The estimates of
419 aromatic SOC exhibited the same geographic trend, with values of $225 \pm 208 \text{ ngC}/\text{m}^3$ over the SCS, 151 ± 177
420 ngC/m^3 over the YBS and $48 \pm 69 \text{ ngC}/\text{m}^3$ over the NWPO. Recent modeling results have also shown that
421 aromatic emissions are the predominant precursors of SOA during springtime in China in comparison with
422 BVOCs and other AVOCs (Han et al., 2016). Among estimates of WSOC_{BB}, the highest values of 209 ± 108
423 ngC/m^3 were recorded over the YBS, followed by comparable levels of $86 \pm 98 \text{ ngC}/\text{m}^3$ (SCS) and 83 ± 145
424 ngC/m^3 (NWPO).

425 In our study, the calculated WSOC_{BB} estimate accounted for $4.1 \pm 5.0\%$ and $3.3 \pm 1.7\%$ of measured OC over the
426 NWPO and YBS, respectively, and these values are higher than that obtained over the ECS during summer
427 (1.4%) (Kang et al., 2018). Estimated SOC from BVOCs accounted for only $1.5 \pm 1.4\%$ and $1.8 \pm 1.7\%$ to the
428 measured OC over the NWPO and YBS, respectively, which is lower than that over ECS (4.21%) (Kang et al.,
429 2018). However, the mean values obtained in this study were similar to the total SOC level estimated using
430 tracers as a proportion of measured WSOC (4%) during a cruise on the North Pacific and Arctic Oceans,
431 supposed that WSOC accounted for half of the total OC in atmospheric particles (Ding et al., 2013).

432 The calculated SOC level derived from organic tracers accounted for less than 8% of total measured OC in these
433 study areas. However, these SOC compounds are expected to derive mainly from photochemical reactions in the
434 gas phase, followed by gas-aerosol partitioning. These compounds likely play an important role in the growth of
435 newly formed particles alongside pre-existing nucleation mode or Aitken mode particles. However, most organic
436 matter detected in bulk samples may originate from primary sources, heterogeneous reactions and in-cloud
437 processing (Ervens et al., 2011; Kanakidou et al., 2005; Nichols, 2016), and these compounds may be major
438 drivers of the direct climate effects of aerosols, rather than indirect climate effects. In the future, a
439 comprehensive combination measurement of organic tracers and organic matter with an aerosol mass

440 spectrometer should be used to elucidate the formation and growth processes of atmospheric nanoparticles.
441



442
443 **Figure 5. Average SOC levels calculated using the tracer-SOC/WSOC method over three marine regions**
444 **(YBS and NWPO in 2014, SCS in 2017) and their contributions based on five organic tracers measured in**
445 **this study.**

446 4. Conclusions

447 This study investigated the geographical distributions of tracer-based organic matter observations in TSP
448 collected over two marginal seas of China and the NWPO in the spring season, when the East Asian monsoon
449 carries biogenic and anthropogenic aerosols over these oceanic zones. We found a significantly large difference

450 in LEVO over the NWPO between two categories of air masses originating from upwind continents or oceanic
451 regions, as Category 1 (continental) contained $13 \pm 18 \text{ ng/m}^3$ and Category 2 (oceanic) had $2.0 \pm 1.8 \text{ ng/m}^3$; the
452 concentrations of LEVO in Category 2 were closer to the low values reported in the literature. This further
453 implied a large increase in continent-derived BB aerosols in marine atmospheres over the NWPO in recent
454 decades, compared to previous studies. An important question is thereby raised, i.e., does a large increase in
455 continent-derived BB aerosols in marine atmospheres over the NWPO occur continuously and largely in recent
456 decades? Combining the L/M ratios of 19 ± 4 over the NWPO with the calculated air mass back trajectories
457 indicates that the increase was very likely associated with enhanced emissions of BB aerosols from wildfires in
458 Siberia and northeastern China. Moreover, the mean level of BB aerosols over the SCS nearly matched that over
459 the NWPO. The contents of LEVO in Category 2 air masses, derived from oceanic zones over the SCS, were
460 comparable with those reported in the literature, but the mean value was only about a quarter of that in Category
461 1, representing air masses from upwind continents. However, the limited data available over the SCS in the
462 literature cannot support inferences about whether BB aerosols emitted from upwind tropical forests have
463 increased in recent decades.

464 The concentrations of SOA_I over the SCS were approximately one order of magnitude greater than those
465 observed over the NWPO and several times larger than those over the YBS. The larger values observed over the
466 SCS in Category 1 than in Category 2 were likely driven by high emissions of isoprene from upwind tropical
467 forests and strong solar radiation. The MTLs dominance of SOA_I over the SCS strongly suggested that SOC
468 from BVOCs was generated primarily under low- NO_x conditions. On the other hand, 2-MGA dominance over
469 the YBS implied that most SOC was generated under high- NO_x conditions. Elevated ratios of 2-MGA/MTLs
470 of >1.5 were obtained for 11 of 19 total samples collected over the NWPO, consistent with those reported in the
471 literature. Larger ratios may be attributed to possible emissions of BVOCs in the presence of BB. However, the
472 comparable concentrations of SOA_I in Category 1 and Category 2 samples collected over the NWPO implied a
473 large contribution of SOA_I from marine sources. The aromatic SOA tracers' levels were highest over the SCS,
474 followed by values obtained over the YBS and NWPO. The high values observed over the SCS may be related
475 to strong solar radiation, but the sources of precursors remain unexplained. Based on the concentrations in
476 Category 1 and 2 air samples collected over the SCS and NWPO, mixed sources of aromatic VOCs should exist,
477 including continent-derived precursors, oil exploration and heavy marine traffic.

478 Over the NWPO and the YBS, the estimated WSOC_{BB} levels were nearly equal to the sum of SOC estimated
479 from the oxidation of aromatics and BVOCs. Over the SCS, SOC estimated from the oxidation of BVOCs was
480 significantly larger than the estimated WSOC_{BB} . The geographical difference may be related to emissions of
481 primary particulate organics and gaseous precursors as well as formation processing of secondary organics in
482 various atmospheres.

483 The atmospheric composition of SOA in different geographical locations is, however, highly complex and is
484 regulated by many factors including local meteorological conditions, anthropogenic emissions, plant species,
485 vegetation cover and regional chemistry, and therefore warrants further quantification and analyses. Particularly,
486 whether BB aerosols and other biogenic organic aerosols in marine atmospheres will continuously increase
487 under warming conditions.

488 **Table 1. Sum of organic tracer contents (ng/m³) at different locations worldwide.**

Site	Date	Sampler	LEVO	SOA _I	SOA _M	SOA _S	SOA _A	Reference
Wakayama, Japan (Forest)	August 20–30, 2010, Day	TSP	2.5±2.1	281±274	54.6±50.2	1.2±1.2		(Zhu et al., 2016a)
	Night		1.1±0.9	199±207	36.3±33.6	0.9±0.8		
Across China	summer 2012	Anderson sampler		123±79	10.5±6.6	5.0±4.0	2.9±1.5	(Ding et al., 2014)
Beijing (PKU) (urban site)	summer 2007	PM2.5	37-148	59±32	30±14	2.7±1.0		(Yang et al., 2016)
Beijing (YUFA) (suburban site)			34-149	75±43	32±14	3.9±1.5		
Shanghai (BS) (Suburban site)	Apr-May 2010	PM2.5	88.8±57.2	3.8±3.9	6.1±3.7	1.0±0.7	1.1±0.7	(Feng et al., 2013)
Shanghai (XJH) (Urban site)			58.3±27.5	2.5±1.7	2.7±1.3	0.4±0.3	0.6±0.4	
Mt. Tai	summer 2014	PM2.5		56.4±45.6	34.4±28.4			(Zhu et al., 2017)
Central Pearl River Delta	fall-winter 2007	PM2.5		30.8±15.9	6.6±4.4	0.5±0.6		(Ding et al., 2011)
Central Tibetan Plateau	2012-2013	Anderson sampler		26.6±44.2	1.0±0.6	0.09±0.1	0.3±0.2	(Shen et al., 2015)
Mumbai, India	winter 2007	PM10		4.1±2.4	29±22		0.6±0.6	(Fu et al., 2016)
	summer 2007			1.1±0.7	9.4±4.7		0.05±0.1	
Alaska	Spring 2009	TSP		2.4	3.6	0.9		(Haque et al., 2016)
	2008-2009	TSP		4.1	2.0	1.5		
SYS	Spring 2017	TSP	9.6±8.6	45±54	3.5±6.0	0.07±0.1	1.8±1.7	This study
YBS	Spring 2014	TSP	21±11	15±16	1.6±2.0	0.1±0.3	1.1±1.4	This study
NWPO	Spring 2014	TSP	8.2±14	2.3±1.6	1.6±2.7	0.05±0.09	0.3±0.5	This study
East China Sea	18 May to 12 June 2014	TSP	0.09–64.3 (7.3)	0.15–64.0 (8.4)	0.26–87.2 (11.6)	0.16–17.2 (2.9)		(Kang et al., 2018)
Arctic to Antarctic	July to September 2008; November 2009 to April 2010	TSP	5.4±6.2	8.5±11	3.0±5.0			(Hu et al., 2013a; Hu et al., 2013b)
North Pacific	2003	TSP		0.5±0.4	0.6±0.4	0.06±0.05	0.002±0.005	(Ding et al., 2013)

**Ocean and the
Arctic**

490 **Data availability.** Most of the data are shown in supplement. Other data are available by contacting the
491 corresponding author.

492 **Supplement.** The supplement related to this article is available.

493 **Author contributions.** XY, TG and JF conceived and led the studies. TG, JW and JF carried out the
494 experiments and analyzed the data. TG and JF interpreted the results. ZG, JF, HG discussed the results and
495 commented on the manuscript. TG prepared the manuscript with contributions from all the co-authors.

496 **Competing interests.** The authors declare that they have no conflict of interest.

497 **Acknowledgements.** This research has been supported by the National Key Research and Development
498 Program in China (No.2016YFC0200504) and the Natural Science Foundation of China (Grant No. 41576118,
499 41473088).

500

501 **References:**

- 502 Ait-Helal, W., Borbon, A., Sauvage, S., de Gouw, J. A., Colomb, A., Gros, V., Freutel, F., Crippa, M., Afif, C.,
503 Baltensperger, U., Beekmann, M., Doussin, J.-F., Durand-Jolibois, R., Fronval, I., Grand, N., Leonardis, T.,
504 Lopez, M., Michoud, V., Miet, K., Perrier, S., Prévôt, A. S. H., Schneider, J., Siour, G., Zapf, P., and Locoge, N.:
505 Volatile and intermediate volatility organic compounds in suburban Paris: variability, origin and importance for
506 SOA formation, *Atmos. Chem. Phys.*, 14, 10439-10464, <https://doi.org/10.5194/acp-14-10439-2014>, 2014.
- 507 Akagi, S. K., Yokelson, R. J., Wiedinmyer, C., Alvarado, M. J., Reid, J. S., Karl, T., Crouse, J. D., and
508 Wennberg, P. O.: Emission factors for open and domestic biomass burning for use in atmospheric models,
509 *Atmos. Chem. Phys.*, 11, 4039-4072, <https://doi.org/10.5194/acp-11-4039-2011>, 2011.
- 510 Andreae, M. O. and Merlet, P.: Emission of trace gases and aerosols from biomass burning, *Global Biogeochem.*
511 *Cy.*, 15, 955-966, 2001.
- 512 Arnold, S. R., Spracklen, D. V., Williams, J., Yassaa, N., Sciare, J., Bonsang, B., Gros, V., Peeken, I., Lewis, A.
513 C., Alvain, S., and Moulin C.: Evaluation of the global oceanic isoprene source and its impacts on marine
514 organic carbon aerosol, *Atmos. Chem. Phys.*, 9, 1253-1262, 2009.
- 515 Bahm, K. and Khalil, M. A. K.: A new model of tropospheric hydroxyl radical concentrations, *Chemosphere*, 54,
516 143-166, <https://doi.org/143-166>, 10.1016/j.chemosphere.2003.08.006, 2004.
- 517 Bao, H., Niggemann, J., Luo, L., Dittmar, T., and Kao, S.: Molecular composition and origin of water-soluble
518 organic matter in marine aerosols in the Pacific off China, *Atmos. Environ.*, 191, 27-35,
519 <https://doi.org/10.1016/j.atmosenv.2018.07.059>, 2018.
- 520 Bonsang, B., Polle, C., and Lambert, G.: Evidence for marine production of isoprene, *Geophys. Res. Lett.*, 19,
521 1129-1132, 1992.
- 522 Bougiatioti, A., Bezantakos, S., Stavroulas, I., Kalivitis, N., Kokkalis, P., Biskos, G., Mihalopoulos, N.,
523 Papayannis, A., and Nenes, A.: Biomass-burning impact on CCN number, hygroscopicity and cloud formation
524 during summertime in the eastern Mediterranean, *Atmos. Chem. Phys.*, 16, 7389-7409,
525 <https://doi.org/10.5194/acp-16-7389-2016>, 2016.
- 526 Broadgate, W. J., Liss, P. S., and Penkett, S. A.: Seasonal emissions of isoprene and other reactive hydrocarbon
527 gases from the ocean, *Geophys. Res. Lett.*, 24, 2675-2678, 1997.

528 Chen, J., Li, C., Ristovski, Z., Milic, A., Gu, Y., Islam, M. S., Wang, S., Hao, J., Zhang, H., He, C., Guo, H., Fu,
529 H., Miljevic, B., Morawska, L., Thai, P., LAM, Y. F., Pereira, G., Ding, A., Huang, X., and Dumka, U. C.: A
530 review of biomass burning: Emissions and impacts on air quality, health and climate in China, *Sci. Total*
531 *Environ.*, 579, 1000-1034, <https://doi.org/10.1016/j.scitotenv.2016.11.025>, 2017.

532 Claeys, M., Graham, B., Vas, G., Wang, W., Vermeylen, R., Pashynska, V., Cafmeyer, J., Guyon, P., Andreae,
533 M. O., Artaxo, P., and Maenhaut, W.: Formation of secondary organic aerosols through photooxidation of
534 isoprene, *Science*, 303, 1173-1176, 2004.

535 Claeys, M., Wang, W., Vermeylen, R., Kourtchev, I., Chi, X., Farhat, Y., Surratt, J. D., Gómez-González, Y.,
536 Sciare, J., and Maenhaut, W.: Chemical characterisation of marine aerosol at Amsterdam Island during the
537 austral summer of 2006–2007, *J. Aerosol Sci.*, 41, 13-22, <https://doi.org/10.1016/j.jaerosci.2009.08.003>, 2010.

538 Davis, D. D., Grodzinsky, G., Kasibhatla, P., Crawford, J., Chen, G., Liu, S., Bandy, A., Thornton, D., Guan, H.,
539 and Sandholm, S.: Impact of ship emissions on marine boundary layer NO_x and SO₂ distributions over the
540 Pacific Basin, *Geophys. Res. Lett.*, 28, 235-238, 2001.

541 Ding, X., Zheng, M., Yu, L., Zhang, X., Weber, R. J., Yan, B., Russell, A. G., Edgerton, E. S., and Wang, X.:
542 Spatial and seasonal trends in biogenic secondary organic aerosol tracers and water-soluble organic carbon in
543 the southeastern United States, *Environ. Sci. Technol.*, 42, 5171-5176, <https://doi.org/10.1021/es7032636>, 2008.

544 Ding, X., Wang, X., and Zheng, M.: The influence of temperature and aerosol acidity on biogenic secondary
545 organic aerosol tracers: Observations at a rural site in the central Pearl River Delta region, South China, *Atmos.*
546 *Environ.*, 45, 1303-1311, <https://doi.org/10.1016/j.atmosenv.2010.11.057>, 2011.

547 Ding, X., Wang, X., Xie, Z., Zhang, Z., and Sun, L.: Impacts of Siberian biomass burning on organic aerosols
548 over the North Pacific Ocean and the Arctic: Primary and secondary organic tracers, *Environ. Sci. Technol.*, 47,
549 3149-3157, <https://doi.org/10.1021/es3037093>, 2013.

550 Ding, X., He, Q., Shen, R., Yu, Q., and Wang, X.: Spatial distributions of secondary organic aerosols from
551 isoprene, monoterpenes, β -caryophyllene, and aromatics over China during summer, *J. Geophys. Res.-Atmos.*,
552 119, 877-891, <https://doi.org/10.1002/2014JD021748>, 2014.

553 Ding, X., Zhang, Y., He, Q., Yu, Q., Shen, R., Zhang, Y., Zhang, Z., Lyu, S., Hu, Q., Wang, Y., Li, L., Song,
554 W., and Wang, X.: Spatial and seasonal variations of secondary organic aerosol from terpenoids over China, *J.*
555 *Geophys. Res.-Atmos.*, 121, 661-678, <https://doi.org/10.1002/2016JD025467>, 2016.

556 Ding, X., Zhang, Y., He, Q., Yu, Q., Wang, J., Shen, R., Song, W., Wang, Y., and Wang, X.: Significant
557 increase of aromatics-derived secondary organic aerosol during fall to winter in China, *Environ. Sci. Technol.*,
558 51, 7432-7441, <https://doi.org/10.1021/acs.est.6b06408>, 2017.

559 Duhl, T. R., Helmig, D., and Guenther, A.: Sesquiterpene emissions from vegetation: a review, *Biogeosciences*,
560 5, 761–777, <https://doi:10.5194/bg-5-761-2008>, 2008,

561 Ehn, M., Thornton, J. A., Kleist, E., Sipilä, M., Junninen, H., Pullinen, I., Springer, M., Rubach, F., Tillmann, R.,
562 Lee, B., Lopez-Hilfiker, F., Andres, S., Acir, I.-H., Rissanen, M., Jokinen, T., Schobesberger, S., Kangasluoma,
563 J., Kontkanen, J., Nieminen, T., Kurtén, T., Nielsen, L. B., Jørgensen, S., Kjaergaard, H. G., Canagaratna, M.,
564 Dal Maso, M., Berndt, T., Petäjä, T., Wahner, A., Kerminen, V.-M., Kulmala, M., Worsnop, D. R., Wildt, J.,
565 and Mentel, T. F.: A large source of low volatility secondary organic aerosol, *Nature*, 506, 476–479,
566 <https://doi.org/10.1038/nature13032>, 2014.

567 Ekström, S., Nozière, B., and Hansson, H.: The Cloud Condensation Nuclei (CCN) properties of 2-methyltetrols
568 and C3-C6 polyols from osmolality and surface tension measurements, *Atmos. Chem. Phys.*, 9, 973-980, 2009.

569 Ervens, B., Turpin, B. J., and Weber, R. J.: Secondary organic aerosol formation in cloud droplets and aqueous
570 particles (aqSOA): a review of laboratory, field and model studies, *Atmos. Chem. Phys.*, 11, 11069-11102,
571 <https://doi.org/10.5194/acp-11-11069-2011>, 2011.

572 Feng, J. L., Guo, Z. G., Zhang, T. R., Yao, X. H., Chan, C. K., and Fang, M.: Source and formation of
573 secondary particulate matter in PM_{2.5} in Asian continental outflow, *J. Geophys. Res.-Atmos.*, 117, D03302,
574 <https://doi.org/10.1029/2011JD016400>, 2012.

575 Feng, J., Li, M., Zhang, P., Gong, S., Zhong, M., Wu, M., Zheng, M., Chen, C., Wang, H., and Lou, S.:

576 Investigation of the sources and seasonal variations of secondary organic aerosols in PM_{2.5} in Shanghai with
577 organic tracers, *Atmos. Environ.*, 79, 614-622, <https://doi.org/10.1016/j.atmosenv.2013.07.022>, 2013.

578 Fraser, M. P. and Lakshmanan, K.: Using levoglucosan as a molecular marker for the long-range transport of
579 biomass combustion aerosols, *Environ. Sci. Technol.*, 34, 4560-4564, <https://doi.org/10.1021/es9912291>, 2000.

580 Fu, P., Kawamura, K., and Miura, K.: Molecular characterization of marine organic aerosols collected during a
581 round-the-world cruise, *J. Geophys. Res.-Atmos.*, 116, D13302, <https://doi.org/10.1029/2011JD015604>, 2011.

582 Fu, P., Aggarwal, S. G., Chen, J., Li, J., Sun, Y., Wang, Z., Chen, H., Liao, H., Ding, A., Umarji, G. S., Patil, R.
583 S., Chen, Q., and Kawamura, K.: Molecular markers of secondary organic aerosol in Mumbai, India, *Environ.
584 Sci. Technol.*, 50, 4659-4667, <https://doi.org/10.1021/acs.est.6b00372>, 2016.

585 Fu, T. M., Cao, J. J., Zhang, X. Y., Lee, S. C., Zhang, Q., Han, Y. M., Qu, W. J., Han, Z., Zhang, R., Wang, Y.
586 X., Chen, D., and Henze, D. K.: Carbonaceous aerosols in China: top-down constraints on primary sources and
587 estimation of secondary contribution, *Atmos. Chem. Phys.*, 12, 2725-2746,
588 <https://doi.org/10.5194/acp-12-2725-2012>, 2012.

589 Gantt, B., Meskhidze, N., and Kamykowski, D.: A new physically-based quantification of marine isoprene and
590 primary organic aerosol emissions, *Atmos. Chem. Phys.*, 9, 4915-4927,
591 <https://doi.org/10.5194/acp-9-4915-2009>, 2009.

592 Generoso, S., Bey, I., Attié, J., and Bréon, F.: A satellite- and model-based assessment of the 2003 Russian fires:
593 Impact on the Arctic region, *J. Geophys. Res.-Atmos.*, 112, D15302, <https://doi.org/10.1029/2006JD008344>,
594 2007.

595 Gordon, H., Kirkby, J., Baltensperger, U., Bianchi, F., Breitenlechner, M., Curtius, J., Dias, A., Dommen, J.,
596 Donahue, N. M., Dunne, E. M., Duplissy, J., Ehrhart, S., Flagan, R. C., Frege, C., Fuchs, C., Hansel, A., Hoyle,
597 C. R., Kulmala, M., Kürten, A., Lehtipalo, K., Makhmutov, V., Molteni, U., Rissanen, M. P., Stozkhov, Y.,
598 Tröstl, J., Tsagkogeorgas, G., Wagner, R., Williamson, C., Wimmer, D., Winkler, P. M., Yan, C., and Carslaw,
599 K. S.: Causes and importance of new particle formation in the present-day and preindustrial atmospheres, *J.
600 Geophys. Res.-Atmos.*, 122, 8739-8760, <https://doi.org/10.1002/2017JD026844>, 2017.

601 Guenther, A., Hewitt, C. N., Erickson, D., Fall, R., Geron, C., Graedel, T., Harley, P., Klinger, L., Lerdau, M.,
602 McKay, W. A., Pierce T., Scholes B., Steinbrecher R., Tallamraju R., Taylor J., and Zimmerman P.: A global
603 model of natural volatile organic compound emissions, *J. Geophys. Res.-Atmos.*, 100, 8873-8892, 1995.

604 Guenther, A., Karl, T., Harley, P., Wiedinmyer, C., Palmer, P. I., and Geron, C.: Estimates of global terrestrial
605 isoprene emissions using MEGAN (Model of Emissions of Gases and Aerosols from Nature), *Atmos. Chem.
606 Phys.*, 6, 3181-3210, 2006.

607 Guenther, A. B., Jiang, X., Heald, C. L., Sakulyanontvittaya, T., Duhl, T., Emmons, L. K., and Wang, X.: The
608 Model of Emissions of Gases and Aerosols from Nature version 2.1 (MEGAN2.1): an extended and updated
609 framework for modeling biogenic emissions, *Geosci. Model Dev.*, 5, 1471-1492,
610 <https://doi.org/10.5194/gmd-5-1471-2012>, 2012.

611 Hackenberg, S. C., Andrews, S. J., Airs, R., Arnold, S. R., Bouman, H. A., Brewin, R. J. W., Chance, R. J.,
612 Cummings, D., Dall'Olmo, G., Lewis, A. C., Minaeian, J. K., Reifel, K. M., Small, A., Tarran, G. A., Tilstone,
613 G. H., and Carpenter, L. J.: Potential controls of isoprene in the surface ocean, *Global Biogeochem. Cy.*, 31,
614 644-662, <https://doi.org/10.1002/2016GB005531>, 2017.

615 Han, Z., Xie, Z., Wang, G., Zhang, R., and Tao, J.: Modeling organic aerosols over east China using a volatility
616 basis-set approach with aging mechanism in a regional air quality model, *Atmos. Environ.*, 124, 186-198,
617 <https://doi.org/10.1016/j.atmosenv.2015.05.045>, 2016.

618 Haque, M. M., Kawamura, K., and Kim, Y.: Seasonal variations of biogenic secondary organic aerosol tracers in
619 ambient aerosols from Alaska, *Atmos. Environ.*, 130, 95-104, 2016.

620 Heald, C. L., Henze, D. K., Horowitz, L. W., Feddema, J., Lamarque, J.-F., Guenther, A., Hess, P. G., Vitt, F.,
621 Seinfeld, J. H., Goldstein, A. H., and Fung, I.: Predicted change in global secondary organic aerosol
622 concentrations in response to future climate, emissions, and land use change, *J. Geophys. Res.-Atmos.*, 113,
623 D05211, <https://doi.org/10.1029/2007JD009092>, 2008.

624 Hennigan, C. J., Sullivan, A. P., Collett Jr., J. L. and Robinson, A. L.: Levoglucosan stability in biomass
625 burning particles exposed to hydroxyl radicals, *Geophys. Res. Lett.*, 37, L09806,
626 <https://doi.org/10.1029/2010GL043088>, 2010.

627 Henze, D. K., Seinfeld, J. H., Ng, N. L., Kroll, J. H., Fu, T.-M., Jacob, D. J., and Heald, C. L.: Global modeling
628 of secondary organic aerosol formation from aromatic hydrocarbons: high-vs. low-yield pathways, *Atmos.*
629 *Chem. Phys.*, 8, 2405-2420, 2008.

630 Hoffmann, D., Tilgner, A., Iinuma, Y. and Herrmann, H.: Atmospheric stability of levoglucosan: A detailed
631 laboratory and modeling study, *Environ. Sci. Technol.*, 44, 694-699, <https://doi.org/10.1021/es902476f>, 2010.

632 Hsiao, T., Ye, W., Wang, S., Tsay, S., Chen, W., Lin, N., Lee, C., Hung, H., Chuang, M., and Chantara, S.:
633 Investigation of the CCN activity, BC and UVBC mass concentrations of biomass burning aerosols during the
634 2013 BASELInE campaign, *Aerosol Air Qual. Res.*, 16, 2742-2756, <https://doi.org/10.4209/aaqr.2015.07.0447>,
635 2016.

636 Hu, D. and Yu, J. Z.: Secondary organic aerosol tracers and malic acid in Hong Kong: seasonal trends and
637 origins, *Environ. Chem.*, 10, 381-394, <https://doi.org/10.1071/EN13104>, 2013.

638 Hu, Q., Xie, Z., Wang, X., Kang, H., He, Q., and Zhang, P.: Secondary organic aerosols over oceans via
639 oxidation of isoprene and monoterpenes from Arctic to Antarctic, *Sci. Rep.-UK*, 3, 2280,
640 <https://doi.org/10.1038/srep02280>, 2013a.

641 Hu, Q., Xie, Z., Wang, X., Kang, H., and Zhang, P.: Levoglucosan indicates high levels of biomass burning
642 aerosols over oceans from the Arctic to Antarctic, *Sci. Rep.-UK*, 3, 3119, <https://doi.org/10.1038/srep03119>,
643 2013b.

644 Hu, Q., Qu, K., Gao, H., Cui, Z., Gao, Y., and Yao, X.: Large increases in primary trimethylaminium and
645 secondary dimethylaminium in atmospheric particles associated with cyclonic eddies in the Northwest Pacific
646 Ocean, *J. Geophys. Res.-Atmos.*, 123, 133-146, <https://doi.org/10.1029/2018JD028836>, 2018.

647 Huang, S., Siebert, F., Goldammer, J. G., and Sukhinin, A. I.: Satellite-derived 2003 wildfires in southern
648 Siberia and their potential influence on carbon sequestration, *Int. J. Remote Sens.*, 30, 1479-1492,
649 <https://doi.org/10.1080/01431160802541549>, 2009.

650 John, J. G., Stock, C. A., and Dunne, J. P.: A more productive, but different, ocean after mitigation, *Geophys.*
651 *Res. Lett.*, 42, 9836-9845, <https://doi.org/10.1002/2015GL066160>, 2015.

652 Kanakidou, M., Seinfeld, J. H., Pandis, S. N., Barnes, I., Dentener, F. J., Facchini, M. C., Van Dingenen, R.,
653 Ervens, B., Nenes, A., Nielsen, C. J., Swietlicki, E., Putaud, J. P., Balkanski, Y., Fuzzi, S., Horth, J., Moortgat,
654 G. K., Winterhalter, R., Myhre, C. E. L., Tsigaridis, K., Vignati, E., Stephanou, E. G., and Wilson, J.: Organic
655 aerosol and global climate modelling: a review, *Atmos. Chem. Phys.*, 5, 1053-1123,
656 <https://doi.org/10.5194/acp-5-1053-2005>, 2005.

657 Kang, M., Fu, P., Kawamura, K., Yang, F., Zhang, H., Zang, Z., Ren, H., Ren, L., Zhao, Y., Sun, Y., and Wang,
658 Z.: Characterization of biogenic primary and secondary organic aerosols in the marine atmosphere over the East
659 China Sea, *Atmos. Chem. Phys.*, 18, 13947-13967, <https://doi.org/10.5194/acp-18-13947-2018>, 2018.

660 Kang, M., Guo, H., Wang, P., Fu, P., Ying, Q., Liu, H., Zhao, Y., and Zhang, H.: Characterization and source
661 apportionment of marine aerosols over the East China Sea, *Sci. Total Environ.*, 651, 2679-2688,
662 <https://doi.org/10.1016/j.scitotenv.2018.10.174>, 2019.

663 Kawamura, K., Hoque, M. M. M., Bates, T. S., and Quinn, P. K.: Molecular distributions and isotopic
664 compositions of organic aerosols over the western North Atlantic: Dicarboxylic acids, related compounds,
665 sugars, and secondary organic aerosol tracers, *Org. Geochem.*, 113, 229-238,
666 <https://doi.org/10.1016/j.orggeochem.2017.08.007>, 2017.

667 Kleindienst, T. E., Jaoui, M., Lewandowski, M., Offenberg, J. H., Lewis, C. W., Bhave, P. V., and Edney, E. O.:
668 Estimates of the contributions of biogenic and anthropogenic hydrocarbons to secondary organic aerosol at a
669 southeastern US location, *Atmos. Environ.*, 41, 8288-8300, <https://doi.org/10.1016/j.atmosenv.2007.06.045>,
670 2007.

671 Lauvset, S. K., Tjiputra, J., and Muri, H.: Climate engineering and the ocean: effects on biogeochemistry and

672 primary production, *Biogeosciences*, 14, 5675-5691, <https://doi.org/10.5194/bg-14-5675-2017>, 2017.

673 Lewandowski, M., Piletic, I. R., Kleindienst, T. E., Offenberg, J. H., Beaver, M. R., Jaoui, M., Docherty, K. S.,
674 and Edney, E. O.: Secondary organic aerosol characterisation at field sites across the United States during the
675 spring-summer period, *Int. J. Environ. Anal. Chem.*, 93, 1084-1103,
676 <https://doi.org/10.1080/03067319.2013.803545>, 2013.

677 Li, L., Tang, P., Nakao, S., Kacarab, M., and Cocker, D. R.: Novel approach for evaluating secondary organic
678 aerosol from aromatic hydrocarbons: unified method for predicting aerosol composition and formation, *Environ.*
679 *Sci. Technol.*, 50, 6249-6256, <https://doi.org/10.1021/acs.est.5b05778>, 2016.

680 Li, M., Zhang, Q., Streets, D. G., He, K. B., Cheng, Y. F., Emmons, L. K., Huo, H., Kang, S. C., Lu, Z., Shao,
681 M., Su, H., Yu, X., and Zhang, Y.: Mapping Asian anthropogenic emissions of non-methane volatile organic
682 compounds to multiple chemical mechanisms, *Atmos. Chem. Phys.*, 14, 5617-5638, 2014.

683 Li, R., Wang, Z., Cui, L., Fu, H., Zhang, L., Kong, L., Chen, W., and Chen, J.: Air pollution characteristics in
684 China during 2015–2016: Spatiotemporal variations and key meteorological factors, *Sci. Total Environ.*, 648,
685 902-915, 2019.

686 Meskhidze, N. and Nenes, A.: Phytoplankton and cloudiness in the Southern Ocean, *Science*, 314, 1419-1423,
687 <https://doi.org/10.1126/science.1131779>, 2006.

688 Mochida, M., Kawamura, K., Fu, P., and Takemura, T.: Seasonal variation of levoglucosan in aerosols over the
689 western North Pacific and its assessment as a biomass-burning tracer, *Atmos. Environ.*, 44, 3511-3518,
690 <https://doi.org/10.1016/j.atmosenv.2010.06.017>, 2010.

691 Murphy, D. M., Chow, J. C., Leibensperger, E. M., Malm, W. C., Pitchford, M., Schichtel, B. A., Watson, J. G.,
692 and White, W. H.: Decreases in elemental carbon and fine particle mass in the United States, *Atmos. Chem.*
693 *Phys.*, 11, 4679-4686, <https://doi.org/10.5194/acp-11-4679-2011>, 2011.

694 Nichols, M. A.: Spatial and temporal variability of marine primary organic aerosols over the global oceans: a
695 review, University of Maryland College Park, 2016.

696 Peñuelas, J. and Staudt, M.: BVOCs and global change, *Trends Plant Sci.*, 15, 133-144,
697 <https://doi.org/10.1016/j.tplants.2009.12.005>, 2010.

698 Rinne, H. J. I., Guenther, A. B., Greenberg, J. P., and Harley, P. C.: Isoprene and monoterpene fluxes measured
699 above Amazonian rainforest and their dependence on light and temperature, *Atmos. Environ.*, 36, 2421-2426,
700 [https://doi.org/10.1016/S1352-2310\(01\)00523-4](https://doi.org/10.1016/S1352-2310(01)00523-4), 2002.

701 Running, S. W.: Is global warming causing more, larger wildfires? *Science*, 313, 927-928,
702 <https://doi.org/10.1126/science.1130370>, 2006.

703 Sharma, S., Lavoué, D., Cachier, H., Barrie, L. A., and Gong, S. L.: Long-term trends of the black carbon
704 concentrations in the Canadian Arctic, *J. Geophys. Res.-Atmos.*, 109, D15203,
705 <https://doi:10.1029/2003JD004331>, 2004.

706 Shen, R., Ding, X., He, Q., Cong, Z., and Wang, X.: Seasonal variation of secondary organic aerosol tracers in
707 Central Tibetan Plateau, *Atmos. Chem. Phys.*, 15, 8781-8793, 2015.

708 Surratt, J. D., Chan, A. W. H., Eddingsaas, N. C., Chan, M., Loza, C. L., Kwan, A. J., Hersey, S. P., Flagan, R.
709 C., Wennberg, P. O., and Seinfeld, J. H.: Reactive intermediates revealed in secondary organic aerosol
710 formation from isoprene, *Proc. Natl. Acad. Sci. U.S.A.*, 107, 6640-6645,
711 <https://doi.org/10.1073/pnas.0911114107>, 2010.

712 Tarvainen, V., Hakola, H., Hellén, H., Bäck, J., Hari, P., and Kulmala, M.: Temperature and light dependence of
713 the VOC emissions of Scots pine, *Atmos. Chem. Phys.*, 5, 989-998, 2005.

714 van der Werf, G. R., Randerson, J. T., Giglio, L., Collatz, G. J., Kasibhatla, P. S., and Arellano Jr, A. F.:
715 Interannual variability in global biomass burning emissions from 1997 to 2004, *Atmos. Chem. Phys.*, 6,
716 3423-3441, 2006.

717 Wang, F., Guo, Z., Lin, T., Hu, L., Chen, Y., and Zhu, Y.: Characterization of carbonaceous aerosols over the
718 East China Sea: The impact of the East Asian continental outflow, *Atmos. Environ.*, 110, 163-173,
719 <https://doi.org/10.1016/j.atmosenv.2015.03.059>, 2015.

720 Warneke, C., Froyd, K. D., Brioude, J., Bahreini, R., Brock, C. A., Cozic, J., de Gouw, J. A., Fahey, D. W.,
721 Ferrare, R., Holloway, J. S., Middlebrook, A. M., Miller, L., Montzka, S., Schwarz, J. P., Sodemann, H.,
722 Spackman, J. R., and Stohl, A.: An important contribution to springtime Arctic aerosol from biomass burning in
723 Russia, *Geophys. Res. Lett.*, 37, L01801, <https://doi.org/10.1029/2009GL041816>, 2010.

724 Yang, F., Gu, Z., Feng, J., Liu, X., and Yao, X.: Biogenic and anthropogenic sources of oxalate in PM_{2.5} in a
725 mega city, Shanghai, *Atmos. Res.*, 138, 356-363, <https://doi.org/10.1016/j.atmosres.2013.12.006>, 2014.

726 Yang, F., Kawamura, K., Chen, J., Ho, K., Lee, S., Gao, Y., Cui, L., Wang, T., and Fu, P.: Anthropogenic and
727 biogenic organic compounds in summertime fine aerosols (PM_{2.5}) in Beijing, China, *Atmos. Environ.*, 124,
728 166-175, 2016.

729 Yao, X., Xu, X., Sabaliauskas, K., and Fang, M.: Comment on “Atmospheric Particulate Matter Pollution during
730 the 2008 Beijing Olympics”, *Environ. Sci. Technol.*, 43, 7589, <https://doi.org/10.1021/es902276p>, 2009.

731 Zhang, H., Surratt, J. D., Lin, Y. H., Bapat, J., and Kamens, R. M.: Effect of relative humidity on SOA
732 formation from isoprene/NO photooxidation: enhancement of 2-methylglyceric acid and its corresponding
733 oligoesters under dry conditions, *Atmos. Chem. Phys.*, 11, 6411-6424,
734 <https://doi.org/10.5194/acp-11-6411-2011>, 2011.

735 Zhang, Q., He, K., and Huo, H.: Policy: cleaning China's air, *Nature*, 484, 161-162, 2012.

736 Zhang, Y., Yang, X., Brown, R., Yang, L., Morawska, L., Ristovski, Z., Fu, Q., and Huang, C.: Shipping
737 emissions and their impacts on air quality in China, *Sci. Total Environ.*, 581-582, 186-198,
738 <https://doi.org/10.1016/j.scitotenv.2016.12.098>, 2017.

739 Zhang, Z., Zhang, Y., Wang, X., Lü, S., Huang, Z., Huang, X., Yang, W., Wang, Y., and Zhang, Q.:
740 Spatiotemporal patterns and source implications of aromatic hydrocarbons at six rural sites across China's
741 developed coastal regions, *J. Geophys. Res.-Atmos.*, 121, 6669-6687, <https://doi.org/10.1002/2016JD025115>,
742 2016.

743 Zhu, C., Kawamura, K., and Kunwar, B.: Effect of biomass burning over the western North Pacific Rim:
744 wintertime maxima of anhydrosugars in ambient aerosols from Okinawa, *Atmos. Chem. Phys.*, 15, 1959-1973,
745 <https://doi.org/10.5194/acp-15-1959-2015>, 2015.

746 Zhu, C., Kawamura, K., Fukuda, Y., Mochida, M., and Iwamoto, Y.: Fungal spores overwhelm biogenic organic
747 aerosols in a midlatitudinal forest, *Atmos. Chem. Phys.*, 16, 7497-7506, 2016a.

748 Zhu, C., Kawamura, K., and Fu, P.: Seasonal variations of biogenic secondary organic aerosol tracers in Cape
749 Hedo, Okinawa, *Atmos. Environ.*, 130, 113-119, <https://doi.org/10.1016/j.atmosenv.2015.08.069>, 2016b.

750 Zhu, Y., Yang, L., Kawamura, K., Chen, J., Ono, K., Wang, X., Xue, L., and Wang, W.: Contributions and
751 source identification of biogenic and anthropogenic hydrocarbons to secondary organic aerosols at Mt. Tai in
752 2014, *Environ. Pollut.*, 220, 863-872, 2017.

753 Zhu, Y., Li, K., Shen, Y., Gao, Y., Liu, X., Yu, Y., Gao, H., and Yao, X.: New particle formation in the marine
754 atmosphere during seven cruise campaigns, *Atmos. Chem. Phys.*, 19, 89-113,
755 <https://doi.org/10.5194/acp-19-89-2019>, 2019.